Drying Technology: An International Journal
Publication details, including instructions for authors and subscription information:
http://www.tandfonline.com/loi/ldrt20

Water Sorption, Glass Transition, and Microstructures of Refractance Window- and Freeze-Dried Mango (Philippine "Carabao" Var.) Powder

O. A. Caparino [a], S. S. Sablani [a], J. Tang [a], R. M. Syamaladevi [a] & C. I. Nindo [b]
[a] Biological Systems Engineering Department, Washington State University, Pullman, Washington, USA
[b] School of Food Science, University of Idaho, Moscow, Idaho, USA
Published online: 18 Nov 2013.

To cite this article: O. A. Caparino, S. S. Sablani, J. Tang, R. M. Syamaladevi & C. I. Nindo (2013) Water Sorption, Glass Transition, and Microstructures of Refractance Window- and Freeze-Dried Mango (Philippine "Carabao" Var.) Powder, Drying Technology: An International Journal, 31:16, 1969-1978, DOI: 10.1080/07373937.2013.805143

To link to this article: http://dx.doi.org/10.1080/07373937.2013.805143

Drying Technology, 31: 1969–1978, 2013

ISSN: 0737-3937 print/1532-2300 online
DOI: 10.1080/07373937.2013.805143

Taylor & Francis
Taylor & Francis Group

Water Sorption, Glass Transition, and Microstructures of Refractance Window– and Freeze-Dried Mango (Philippine "Carabao" Var.) Powder

O. A. Caparino,[1] S. S. Sablani,[1] J. Tang,[1] R. M. Syamaladevi,[1] and C. I. Nindo[2]
[1]*Biological Systems Engineering Department, Washington State University, Pullman, Washington, USA*
[2]*School of Food Science, University of Idaho, Moscow, Idaho, USA*

Water sorption isotherms, glass transition, and microstructures of Refractance Window (RW)– and freeze-dried Philippine "Carabao" mango powders were investigated. Water sorption isotherms were developed by the isopiestic method, while thermal transition of the powders, at various water activities ($a_w = 0.11$–0.86), was determined using differential scanning calorimetry (DSC). The sorption isotherms of RW- and freeze-dried (FD) mango powders exhibited a type III sigmoidal curve, showing higher and lower adsorption capacities above and below 0.5 a_w, respectively. A significant difference ($p < 0.05$) in water content of RW- and freeze-dried mango powders for equivalent water activities was obtained above 0.5 a_w. The onset glass transition temperature (T_{gi}) of RW- and freeze-dried mango powder solids decreased as the water content increased. There were no significant differences ($p \geq 0.05$) in T_{gi} of RW- and freeze-dried mango powder solids at constant water activities, except for $a_w = 0.86$. Microscopic examination of mango powders indicated that freeze-dried mango powders exhibited greater surface area and porosity in comparison to RW-dried mango powders.

Keywords Freeze drying; Glass transition temperature; Mango powder; Refractance window drying; Scanning electron microscopy; Water adsorption

INTRODUCTION

Mango (*Mangiferaindica L.*) is one of the most important fruit trees in tropical countries. In the Philippines, mango ranks third among fruit crops produced, after banana and pineapple, based on export volume and value, with over one million metric tons harvested in 2007 according to the Philippine Bureau of Statistics.[1] The Carabao variety popularly known as "Philippine Super Mango" is the dominant variety that accounts for 73% of the country's production.[1] Although many food companies produce various products from mango, such as puree, juice and concentrate, there is a continuing interest in efforts to process it into powder to make it more stable. Mango powders can be utilized in various innovative formulations that create opportunities for applications in a wide range of products, such as dry beverage mixes, health drinks, baby foods, sauces, marinades, confections, yogurt, ice cream, nutrition bars, baked goods, and cereals.[2] However, the processing of mango powder presents many research challenges in drying operations because of its inherent sticky characteristics attributed to the presence of low molecular weight sugars such as sucrose, fructose, glucose, and organic acids.[3]

Water activity is a widely accepted concept and is frequently used as a parameter to predict the microbial, chemical, and physical stability of food products over time. Water activity influences microbial growth, lipid oxidation, non-enzymatic and enzymatic activities.[4] Expressing the relation between water activity and equilibrium water content in a graphical form at a fixed temperature produces a water sorption isotherm. Sorption isotherms are used to relate physical, chemical, and microbiological stability, all of which are important parameters during drying, packaging, and storage of food products.

Monolayer water content is another useful value that relates to the amount of bound water in a solid material. It normally varies between 0.04–0.11 kg H_2O/kg dry solids for several dried foods.[5] This low water content does not support microbial reactions, and hence contributes to food product stability.[4] Since microstructure and morphology of most biomaterials are altered during drying processes, investigations of the microstructures of food powders may provide some useful insights into the sorption behavior of a specific product.

Many authors[4,6] have discussed limitations in applying a water activity concept for predicting food stability, due to the following concerns: 1) not all food products are in an equilibrium state, and measurement of water activity at a specific time might not describe the steady-state

Correspondence: Juming Tang, Biological Systems Engineering Department, Washington State University, 208 LJ Smith Hall, Pullman, WA 99164-6120, USA; E-mail: jtang@wsu.edu or Caleb Nindo, School of Food Science, University of Idaho, Ag Sci 111, 875 Perimeter Dr, Moscow, ID 83844-2312, USA; E-mail: cnindo@uidaho.edu

conditions of these products; 2) critical limits of water activity might provide inaccurate values as affected by pH, salt, antimicrobial agent, and pre-treatments; and 3) water activity cannot safely tell whether the water present in food is immobilized or not water. In consideration of these limitations, a glass transition temperature concept was applied to the food system. It is hypothesized that the glassy state can greatly enhance the stability of food because diffusion controlled reactions rates are significantly reduced.[4,7] Both the water activity and glass transition concepts have been proposed to predict deterioration, stability, and shelf-life of food because, in many instances, glass transition alone does not work.[8] Glass transition temperature as a function of water activity or water content can be used to construct a state diagram for a particular food system and there is evidence from previous studies that using the state diagram can better assist the food industry in determining the stability of their products.[9] Several studies related to the interactions of water activity, water content, and glass transition temperature of agricultural and fishery products have been reported.[10,11]

Glass transition temperature greatly influences the stability of food since below this temperature water is kinetically immobilized, restricting it from participating in the reactions.[12,40] Depending on the temperature and rate of water removal during drying, production of powder from a sugar-rich fruit such as mango may cause loss of quality or degradation during drying and subsequent storage. However, there is little or no published information about sorption isotherms, glass transition and state diagrams of freeze-dried (FD) and Refractance Window–dried (RW) mango powder. The objectives of this study were to develop sorption isotherms, determine glass transition temperatures, and examine the microstructures of mango powder dried using Refractance Window and freeze drying methods.

MATERIALS AND METHODS

Preparation of Mango Powder and Packaging

Frozen mango puree, processed from the "Carabao" variety that is dominant in the Philippines, was acquired from Ramar Foods International (Pittsburg, CA). The puree was thawed overnight at ~22°C and blended for five minutes to a uniform consistency using a bench-top blender (Oster Osterizer, Mexico) at the lowest speed setting. The puree with initial water content of 6.52 ± 0.12 kg water/kg dry solids was dried to below 0.03 kg water/kg dry solids using Refractance Window® drying or freeze-drying methods. A pilot-scale Refractance Window® dryer (with an effective drying area of 1.10 m^2) developed by MCD Technologies, Inc. (Tacoma, WA) was used in the experiment.[13] The dryer has the following components: a water pump, a hot water tank, a heating unit, two water flumes, a hood with suction blowers and exhaust fans, a conveyor belt made of "Mylar®" (polyethylene terephthalate) plastic, a spreader at the inlet section, and a scraper at the end section of the dryer. During the drying operation, circulating hot water between 95–97°C was maintained to continuously transfer thermal energy to the puree through the plastic conveyor interface. An average air velocity of 0.7 m/s with a relative humidity ranging from 50–52% was applied on the surface of the puree to facilitate moisture removal.[14,13] Freeze drying was carried out using a laboratory freeze dryer (Freeze Mobile 24, Virtis Company, Inc., Gardiner, NY) after thawing the mango puree and pouring it into stainless pans to form a layer of 15 mm. The samples were placed at −25°C for 24 hours before being transferred to the freeze dryer. The vacuum pressure of the dryer was set at 20 Pa, the plate temperature was 20°C, and the condenser was at −60°C.[13]

The resulting RW and FD mango flakes or sheets were collected and packed in leak-proof Ziploc® plastic bags and double packed in aluminum-coated polyethylene bags. All packaged samples were flushed with nitrogen gas to prevent oxidation, heat sealed, and stored at −35°C until further analyses. One hundred grams of dried mango flakes or sheets obtained from the RW and freeze-drying processes were ground using a mortar and pestle and were sieved using sizes 60 and 80 (American Society for Testing and Materials, ASTM) to obtain particle sizes between 180–250 μm.[15] This range of particle size was selected for better interpretation of the microstructures of mango powders and for convenience during DSC loading. The prepared samples were used for water sorption, thermal, and microstructures experiments.

Measurements of Residence Time, Product Temperature, and Water Content

For Refractance Window drying, the residence time to dry the mango puree was determined by monitoring the time taken by the thinly spread mango puree to travel from the inlet to the outlet section of the plastic conveyor belt. The product temperature was measured with an infrared temperature sensor (Raytek MT6 Mini, Santa Cruz, CA) on approximately three gram- samples scraped off along the travel direction of the belt at different locations within the drying section. In the freeze-drying method, the residence time required to lower the initial water content to a similar water content level as that of RW drying was determined when the vacuum pressure of the freeze dryer had dropped to 4 Pa. The product temperature was measured using pre-calibrated Type-T thermocouple sensors, which were connected to a data acquisition device (USB-PC Measurement Computing Corp., Norton, MA) equipped with monitoring software. The water content of mango

puree, RW- and freeze-dried mango flakes or powders was determined using the standard oven method at 70°C and 13.3 kPa for 24 hours.[16] Measurements for process time and product temperature were made in duplicate while water content was in triplicate.

Determination of Sorption Isotherms

An adsorption isotherm was developed using the isopiestic method according to Speiss and Wolf.[17] The RW- and freeze-dried mango powders were placed in airtight humidity jars and equilibrated at room temperature (~23°C) for 35 days using saturated salt solutions to provide constant water activity. The saturated salt solutions used were LiCl, CH_3COOK, MgCl, K_2CO_3, $MgNO_3$, $NaNO_2$, NaCl, and KCl (Fisher Scientific, Houston, TX), with corresponding known relative humidity of 11.3%, 22.5%, 32.8%, 43.2%, 52.9%, 65.8%, 75.0%, and 86.0% at 23.0°C, respectively. To prevent microbial growth in the samples, a small amount of thymol was added in a small uncapped bottle and placed together with the samples inside the airtight humidity jars. The water content of the equilibrated RW- and freeze-dried mango powders was determined using the standard oven method at 13.3 kPa and 70°C and for 24 h.[16]

Several water sorption isotherm model equations, such as Brunauer-Emmett-Teller (BET),[18,42] Henderson equation,[19] Smith equation,[20] and Guggenheim-Andersen-de Boer (GAB),[21,22] have been applied to determine monolayer water content in foods. For RW- and freeze-dried mango powder, we used the BET and GAB models.[22] The BET isotherm is applicable between water activities of 0.05 and 0.45, while GAB is applicable for a wide range of water activities between 0 and 0.95.[23,24,12] The BET equation[21] is expressed as:

$$M_w = \frac{M_b B a_w}{[(1 - a_w)(1 + (B - 1)a_w)]} \quad (1)$$

where M_w is the water content (kg water/kg dry solids); M_b is the BET monolayer water content (dry basis); B is a constant related to net heat of sorption.

The GAB equation[21] is expressed as:

$$M_w = \frac{M_g C K a_w}{[(1 - K a_w)(1 - K a_w + C K a_w)]} \quad (2)$$

where M_w is the water content (kg water/kg dry solids); M_g is the GAB monolayer water content (dry basis); C is a constant related to the monolayer heat of sorption; and K is a factor related to the heat of sorption of the multilayer and its value varies from 0.7 to 1.0.

Estimation and optimization of parameters in BET and GAB equations were done using Microsoft Excel® software. Duplicate samples were measured and analyzed.

Thermal Transitions

The glass transition temperatures of RW- and freeze-dried mango powder solids with water content ranging from 0.074–0.097 kg solid/kg mango powder were determined using DSC Q2000 (TA Instruments, New Castle, DE, USA) following the procedure described in Syamaladevi et al.[10] The calorimeter was calibrated for heat flow and temperature using standard indium and sapphire. An empty aluminum pan was used as a reference for each sample test. Ten to 12 milligrams of the equilibrated mango powders were sealed in an aluminum pan (volume of 30 μL), cooled from 25°C to −90°C using liquid nitrogen, and equilibrated for 10 min. The equilibrated samples were scanned to 70°C and then cooled down to 25°C. Scanning of all samples was carried out using the same heating or cooling rate of 5°C/min.[10] A nitrogen carrier gas was purged at a flow rate of 50 ml/min. The state diagram was determined by DSC thermo grams using Universal Analysis 2000 software (TA Instruments, Newcastle, DE, USA). Glass transition temperature (T_g) of the mango powder solids was determined by finding the vertical shift in the heat flow-temperature diagram. Glass transition temperatures of mango powder solids at different water activity levels and equilibrium water content were measured in duplicate.

Plasticization behavior of mango constituents by water was predicted using the Gordon and Taylor equation,[19] expressed as:

$$T_{gm} = \frac{X_s T_{gs} + k X_w T_{gw}}{X_s + k X_w} \quad (3)$$

where X_w, $X_s T_{gm}$, T_{gs}, and T_{gw} are the mass fraction of water, glass transition temperatures of the mixture, solids, and water, respectively. The k is the Gordon-Taylor parameter calculated from the ratio of specific heats of solids to water. The glass transition curve was established by extrapolating the T_g values of the samples using the glass transition temperature of water ($T_g = -135$°C) as the lower end temperature limit. The glass transition temperature of samples at zero water (T_{gs}) and k values were calculated by applying nonlinear regression.[11]

Microstructures of Mango Powders

A small quantity of mango powders (with particle sizes between 180 to 250 μm) was mounted on 12.7-mm-diameter aluminum stubs and coated with a fine layer of gold (15 nm) using a Sputter gold coater (Technics Hummer V, Anatech, San José, CA). The samples were examined by a scanning electron microscope (Hitachi S-570, Hitachi Ltd., Tokyo, Japan) camera operated at an accelerating voltage of 20 kV. The microstructures were

photographed at a magnification of 300 x and 1,000 x at a scale of 100 μm and 30 μm, respectively.

Statistical Analysis

All experiments were carried out at least in duplicate, and the results were analyzed using SASgeneral linear model procedure (SAS Institute Inc., Cary, NC) and Tukey-honest significant difference test with a confidence interval of 95% used to compare the means.

RESULTS AND DISCUSSION

Drying Time, Water Content, and Product Temperature

The RW drying of mango puree from an initial water content of 6.52 ± 0.12 kg water/kg mango solids to below 0.05 kg water/kg mango solids was accomplished in about three minutes compared to freeze drying, which took 31 hours (Table 1). The temperature of the mango puree during the RW drying experiment (74 ± 2°C) was maintained at that level by hot water (95–97°C) circulating under the belt. The relative humidity was 50–52% (Table 1). On the other hand, the product temperature obtained during freeze drying was 20 ± 0.5°C, similar to the chamber temperature of the freeze dryer at 20 Pa.

Water Sorption Isotherms

The equilibrium condition of the mango powders was achieved after 35 days of storage at 23°C and at different relative humidities or water activities. As shown in Fig. 1, it is evident that water activity and equilibrium water content of the product have a direct relationship; i.e., as water content increases, there is a corresponding increase of water activity. Both the sorption isotherms for RW- and freeze-dried powder followed type III (J-shape) behavior, typical of sugar-rich products.[24] For a food material with type III isotherm, a lower rate of moisture gain at the initial water activity levels is observed.[24,42] This water sorption behavior is similar to sorption curves observed for other products with high sugar contents and amorphous dried materials such as osmo-dried star apple and mango,[23] freeze-dried blueberries,[25] air-dried grapefruits,[26] apple puree powders,[27] and freeze-dried mango pulp.[28] Both the RW- and freeze-dried mango powders tended to adsorb small amounts of water at low water activity (<0.5), due to possible local dissolution of sugars and formation of new active sites.[23] On the other hand, at higher water activity ($a_w > 0.5$) a sharp increase was shown due to gradual dissolutionand complete exudation of sugar present in mango as a result of its crystalline structure breakdown and the appearance of more active sites.[28,23]

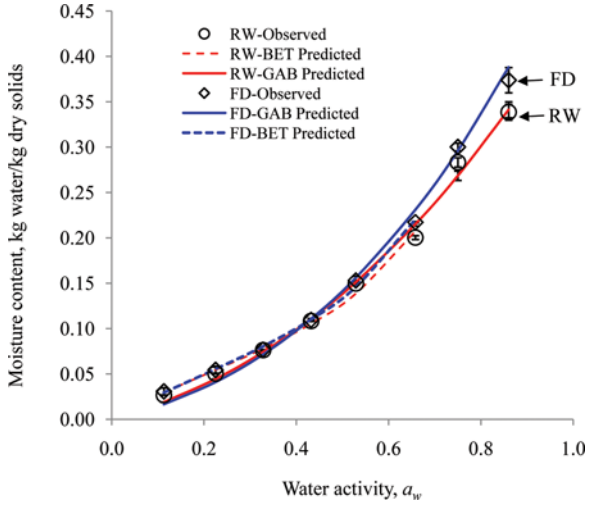

FIG. 1. Water adsorption isotherm data for Refractance Window– and freeze-dried mango powders at 23°C, with fitted curvesusing GAB and BET models (color figure available online).

A significant difference ($p < 0.05$) in water content of RW-dried and freeze-dried mango powders for equivalent water activities was observed at a_w above 0.5 (Fig. 1). This indicates that water adsorption capacities of freeze-dried mango powder were higher than RW-dried mango powder at water activity above 0.50, as shown by the significant increase in water content in freeze-dried mango powders.

BET and GAB models were fitted to the water activity/water content data for mango powders obtained by the two drying methods investigated ($R^2 = 0.972$–0.986) (Fig. 1). The monolayer (monomolecular) water content is considered the lowest practical limit for most drying applications, below which drying processes become inefficient. This limit is also widely accepted as the safest water content for maintaining food stability over a long period of storage. Similar BET monolayer water contents (M_b) were obtained

TABLE 1
Temperature, retention time, and water content of mango puree, Refractance Window– and freeze-dried mango powders

Product	Product temperature (°C)	Retention time (min)	Water content (kg water/kg dry solids)
Fresh puree	–	–	6.518 ± 0.123
RW	74 ± 2	3 ± 0.01	0.017 ± 0.001
FD	20 ± 1	$1{,}860 \pm 85$	0.023 ± 0.002

RW: Refractance Window-dried mango powder; FD: Freeze dried mango powder.

for RW (0.081 kg H_2O/kg dry solids) and freeze-dried (0.087 kg H_2O/kg dry solids) mango powders by nonlinear regression analyses (Table 2). The GAB monolayer water content (M_g) of RW- and freeze-dried mango powder was 0.078 kg H_2O/kg dry solids and 0.045 kg H_2O/kg dry solids, respectively (Table 2). The smaller GAB monolayer value of freeze-dried mango powder in comparison to RW mango powder may be attributed to the overlapping of predicted water content values below 0.5 a_w and the significant difference in water content values above 0.5 a_w (Fig. 1). The obtained BET and GAB monolayer values in the present experiments are within the range of mono layer values for several dehydrated fruit products between 0.026 and 0.185 kg H_2O/kg dry solids (Table 2).[10,23,27,28] The variations in monolayer water content of sugar-rich materials could be attributed to the different drying processes applied and sugar composition of these fruits.

Glass Transition Temperature

The onset, mid-, and end glass transition temperatures (T_{gi}, T_{gm}, and T_{ge}) were recorded in this study to better define the T_g since there is no consensus definition on either one of those temperatures being the transition point in a DSC curve.[6] However, some authors[30] have used T_{gm} to describe the glass transition of different products. Based on the premise that glass transition temperature starts at $T_{gi,}$, we considered this value as the safest T_g for storage of mango powder, and subsequently used it to establish the relationship between T_g, water activity, and water content. The T_{gi} of both the RW- and freeze-dried mango powder solids obtained by a single-scan DSC analysis shifted toward lower temperatures as the water activity increased (Fig. 2). The inverse relationship of glass transition and water activity in this particular study is attributed to the strong plasticizing effect of water ($T_g = -135°C$) on amorphous components of the food matrix.[30,31] The thermograms of RW- and freeze-dried mango powders conditioned at water activities ($a_w = 0.11$–0.86) showed that one transition wherein no crystalline peak was observed in the DSC thermogram. Similar thermogram behavior was reported for dried fruits containing high sugars, such as raspberry,[10] pineapple,[32] and strawberries.[33] No significant differences in the initial glass transition temperatures (T_{gi}) of RW-dried and freeze-dried mango powder solids were observed for equivalent water activities, except for $a_w = 0.86$ (Table 3) ($p < 0.05$). The T_{gm} values of RW and freeze-dried mango powder solids decreased from $35.6 \pm 1.5°C$ to $-61.4 \pm 3.3°C$ and $39.7 \pm 2.2°C$ down to $-67.8 \pm 1.6°C$ as the water content increased from 0.03 ± 0.001 to 0.34 ± 0.005 kg water/kg dry solids and 0.03 ± 0.005 to 0.37 ± 0.014 kg water/kg dry solids, respectively (Table 3). The lowest initial glass transition temperatures (T_{gi}) measured for RW- and freeze-dried mango powder solids with 0.86 a_w were $-65.3°C$ and

TABLE 2
Measured BET and GAB parameters of mango powders and other sugar-rich fruits

		BET Model parameters			GAB Model parameters			
Product	Air Temperature	*Mg* (kg H_2O/kg dry solids)	B	R^2	*Mg* (kg H_2O/kg dry solids)	C	K	R^2
RW-dried mango[a]	23°C	0.081	3.77	0.984	0.078	8.75	0.203	0.986
Freeze-dried mango[a]	23°C	0.087	3.35	0.986	0.045	8.08	0.315	0.972
Freeze-dried mango[b]	25°C	0.136	−19.54	0.971	0.124	0.136	−19.54	0.986
Osmo-oven-dried mango[c]	25°C	NA	NA	NA	0.166	NA	NA	NA
Dehydrated mango[d]	40°C	0.129	94.30	NA	0.096	0.129	94.30	NA
Dehydrated pineapple[d]	40°C	0.266	24.45	NA	0.185	0.266	24.45	NA
Dehydrated banana[d]	40°C	0.181	74.49	NA	0.108	0.181	74.49	NA
Freeze-dried raspberry[e]	23°C	0.056	NA	NA	0.074	0.056	NA	NA
Freeze-dried apple[f]	25°C	NA	NA	NA	0.120	NA	NA	NA
Air-dried apple[f]	25°C	NA	NA	NA	0.125	NA	NA	NA

[a]Present study.
[b]Rangel–Marrón et al.[28]
[c]Falade and Aworth.[23]
[d]Talla et al.[45]
[e]Syamaladevi et al.[10]
[f]Jakubczyk et al.[27]
NA - Not available.
M_g - Monolayer moisture content.

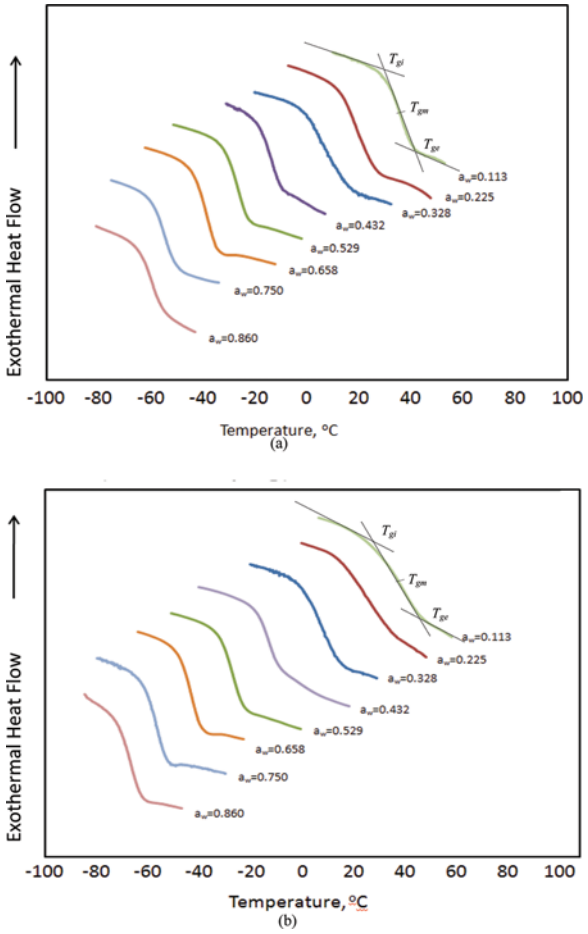

FIG. 2. Glass transition temperatures of Refractance Window–dried (a) and freeze-dried (b) mango powders equilibrated over selected water activity (scan rate of 5°C/min) (color figure available online).

−72.2°C, respectively, possibly due to plasticization by the large amount of water. The highest initial glass transition temperature was observed for RW-dried (30.6°C) and FD-dried (33.4°C) mango powder solids with water activity of 0.113, due to greater dry solid concentration.[9,32] The glass transition curve was fitted with the Gordon-Taylor (G-T) equation, and was extrapolated to the glass transition temperature of water ($T_g = -135$°C) (Fig. 3). The glass transition temperature of mango powder solids at zero water (T_{gs}) and constant k values was calculated by applying nonlinear regression, as described in Sablani and others.[11] The glass transition temperature for RW- and freeze-dried mango powder solids at zero water (T_{gs}), when fitted to the Gordon-Taylor model, was 55.8 and 63.6°C, respectively (Fig. 3). These values were close to the glass transition temperature of vacuum-dried mango (unspecified variety) of 62°C, as reported by Jaya and Das.[34] Apparently, the low T_{gs} of RW- and freeze-dried mango powder solids is mainly due to the high concentration of sucrose in mango. Mango is rich in sugars, mainly sucrose (0.060–0.095 kg/kg of pulp), fructose (0.025–0.027 kg/kg of pulp) and glucose (0.007–0.047 kg/kg of pulp).[34] The glass transition temperatures of dry sucrose, fructose, and glucose were reported to be 62°C, 5°C, and 32°C, respectively.[30,35] Telis and Sobral[32] observed a higher T_{gs} for freeze-dried tomato than air-dried tomato, attributed to the structural differences between freeze-dried and air-dried products.

Sorption isotherms and state diagrams of RW and freeze-dried mango powders were combined to examine their relationships in terms of product stability during storage (Figs. 4 and 5 and Table 4). It can be seen from the figures that the relationships among glass transition temperature, water activity, and water content for mango powder solids obtained by the two drying methods revealed

TABLE 3
Glass transition temperatures and moisture contents of Refractance Window– and freeze-dried powders at water activity ($0.113 \le a_w \le 0.860$)

Water activity	T_{gi} (°C)		T_{gm} (°C)		T_{ge} (°C)		Water content (kg water/kg dry solids)	
	RW	FD	RW	FD	RW	FD	RW	FD
0.113	30.6 ± 1.5^{a}	33.4 ± 3.4^{a}	35.6 ± 1.5^{j}	39.7 ± 1.2^{j}	39.2 ± 1.2^{1}	46.1 ± 0.9^{2}	0.03 ± 0.001^{13}	0.03 ± 0.005^{13}
0.225	13.9 ± 0.1^{b}	13.6 ± 6.1^{b}	20.3 ± 1.3^{k}	27.2 ± 5.3^{1}	24.6 ± 0.8^{3}	35.2 ± 4.2^{4}	0.05 ± 0.001^{14}	0.05 ± 0.002^{14}
0.328	-3.3 ± 0.9^{c}	0.2 ± 2.5^{c}	1.8 ± 0.2^{m}	5.9 ± 3.3^{m}	5.9 ± 0.2^{5}	10.8 ± 2.6^{6}	0.08 ± 0.001^{15}	0.08 ± 0.001^{15}
0.432	-17.5 ± 0.2^{d}	-16.6 ± 0.5^{d}	-12.7 ± 0.5^{n}	-13.1 ± 0.5^{n}	-10.1 ± 0.6^{7}	-9.7 ± 0.3^{7}	0.11 ± 0.001^{16}	0.11 ± 0.001^{16}
0.529	-31.9 ± 0.9^{e}	-31.4 ± 0.4^{e}	-26.7 ± 0.6^{o}	-27.3 ± 0.1^{o}	-23.3 ± 0.1^{8}	-23.9 ± 0.5^{8}	0.15 ± 0.002^{17}	0.15 ± 0.001^{17}
0.658	-45.3 ± 3.2^{f}	-47.4 ± 0.6^{f}	-40.6 ± 2.9^{p}	-42.4 ± 0.6^{p}	-37.6 ± 3.3^{9}	-39.4 ± 0.7^{9}	0.20 ± 0.001^{18}	0.22 ± 0.001^{19}
0.750	-56.6 ± 3.5^{g}	-60.7 ± 0.1^{g}	-52.3 ± 2.8^{q}	-57.0 ± 1.7^{r}	-49.7 ± 2.7^{10}	-53.3 ± 1.0^{10}	0.28 ± 0.003^{20}	0.30 ± 0.004^{21}
0.860	-65.3 ± 1.9^{h}	-72.2 ± 1.4^{i}	-61.4 ± 3.3^{r}	-67.8 ± 1.6^{s}	-57.6 ± 1.8^{11}	-64.7 ± 1.5^{12}	0.34 ± 0.005^{22}	0.37 ± 0.014^{23}

$^{(a–s);\ (1–23)}$Different superscript letters and numbers represent statistical significant differences of glass transition temperatures of RW- and freeze-dried mango powders at various water activities ($a_w = 0.113$–0.86).

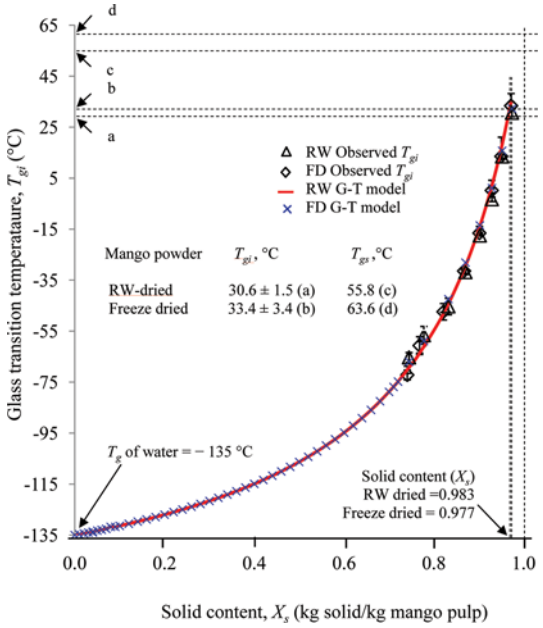

FIG. 3. State diagram of Refractance Window (RW) and freeze-dried (FD) mango powders. The onset (T_{gi}) and solids (T_{gs}) glass transition temperatures of RW- and freeze-dried mango powders are represented by letters (a & b) and (c & d), respectively (color figure available online).

certain variations. The stable temperature range predicted by the glass transition model based on the sorption isotherms underestimates the stable temperature range. For example, in the case of RW-dried mango powder solids, the critical glass transition temperature based on the sorption isotherm at 23°C was smaller than the stable

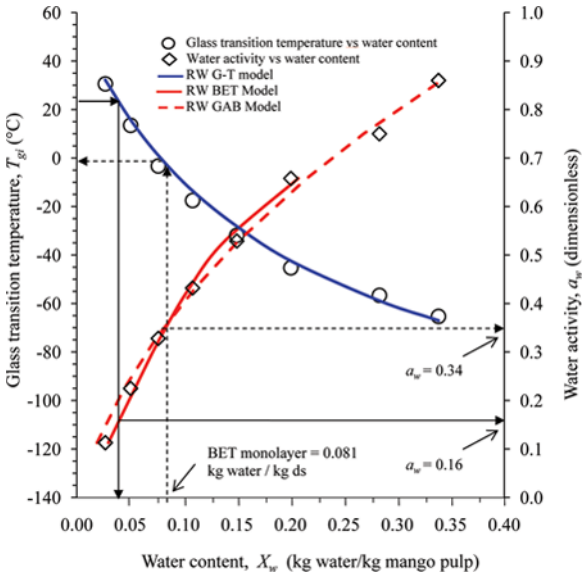

FIG. 4. Water plasticization and sorption characteristics of Refractance Window–dried (RW) mango powders showing water activity, water content, and glass transition temperature (color figure available online).

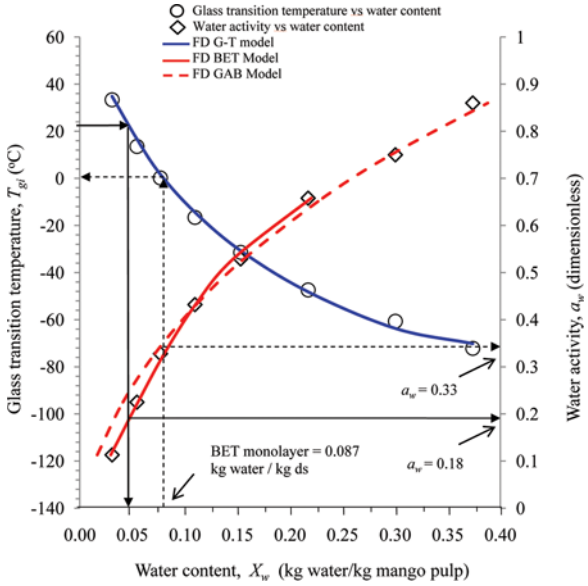

FIG. 5. Water plasticization and sorption characteristics of freeze-dried (FD) mango powders showing water activity, water content, and glass transition temperature (color figure available online).

temperature range. The RW-dried mango powders are stable at a BET monolayer water content of 0.081 (Fig. 4). However, by using the same water content, the T_g value as presented in the glass line (dotted arrow lines) was predicted at lower storage temperature (0°C). The T_g-water activity relationship presented in Table 4 suggests that RW-dried mango powder at water content of 0.017 kg water/kg mango pulp is stable when stored at temperatures no higher than 23°C. The water activity of RW-dried mango powder ($a_w = 0.16$) obtained in sorption isotherms predicted at 23°C is lower than the monolayer water activity ($a_w = 0.34$). This indicates that mango powder with $a_w \leq 0.34$ is safe to store at 23°C or lower. Other authors working on sugar-rich materials made similar observations.[10,11,32,33]

On the other hand, the critical glass transition temperature for freeze-dried mango powder solids appeared to be similar to the "stable condition" associated with its monolayer water content (Fig. 5). It was observed that freeze-dried mango powder is stable at 0.087 kg water/kg dry solids when stored at 23°C. Apparently, when using the same lower limit water content, the glass transition temperature did not change significantly as shown in the glass line or dotted lines (23°C). Analysis of the water content and glass transition temperature data (Table 4) shows clearly that freeze-dried mango powder with 0.087 kg water/kg dry solids is stable at 23°C. At the same temperature, the sorption isotherm model predicts a water activity of 0.18, slightly lower than the monolayer water activity ($a_w = 0.33$) for safe storage of freeze-dried mango powder. In the current study, RW-dried and freeze-dried

TABLE 4
Evaluating water sorption isotherm and glass transition models of Refractance Window– and freeze-dried mango powders using BET monolayer water content

		Sorption isotherm model			Glass transition model		
Product	Temp. (°C)	BET monolayer water content (kg water/ kg mango)	a_w corresponding to monolayer water content (fraction)	T_g from glass transition model (°C)	T_g (°C)	Water content (kg/kg mango	a_w corresponding to monolayer water content (fraction)
RW-dried mango powder	23	0.081	0.34	0	23	0.017	0.16
Freeze-dried mango powder	23	0.087	0.33	0	23	0.023	0.18

mango powders exhibited similar sorption and glass transition characteristics as other high sugar materials. Sablani et al.[11] reported that the glass transition concept often underestimates the safe temperature for dehydrated fruits with sugar content. Further studies on physicochemical changes, such as degradation of bioactive compounds (β-carotene and vitamin C) in dehydrated mango stored at the selected water contents/activities, may explain whether it is appropriate to apply water activity or glass transition temperature concepts in these situations.

Microstructures

The microstructures of mango powders and similar fruits depend on the drying method applied.[41,43,44] The RW-dried mango powder appeared as smooth flakes with nearly uniform thickness (Fig. 6a,b).The uniformity of the flake thickness was the result of a controlled feeding of mango puree using a spreader bar at the inlet section of the RW dryer. During the drying, the thinly spread mango puree on the surface of the plastic film conveyor remained virtually undisturbed as it moved toward the discharge end of the dryer, hence producing a continuous sheet with uniform thickness. Breaking the RW-dried mango flakes into powder form produced irregularly shaped particles while the thickness was unchanged. The edges of the resulting single particles (miniature flakes) were smooth, hence were more flowable and possibly would lead to low susceptibility to oxidation because of the smaller surface area.

The microstructures of freeze-dried mango powder had a skeletal structure with evident void spaces previously occupied by ice prior to freeze drying (Fig. 6c,d). This is because the absence of a liquid phase in the material during the freeze-drying process suppressed the transfer of liquid water to the surface and the ice converting to vapor without first becoming liquid.[36] In effect, the collapse and shrinkage of the product was prevented, thereby resulting in a porous dried material.[5]

Collapse and shrinkage phenomena have been proposed to have relationships to the glass transition temperature.[37,43] Achanta and Okos[38] hypothesized that shrinkage

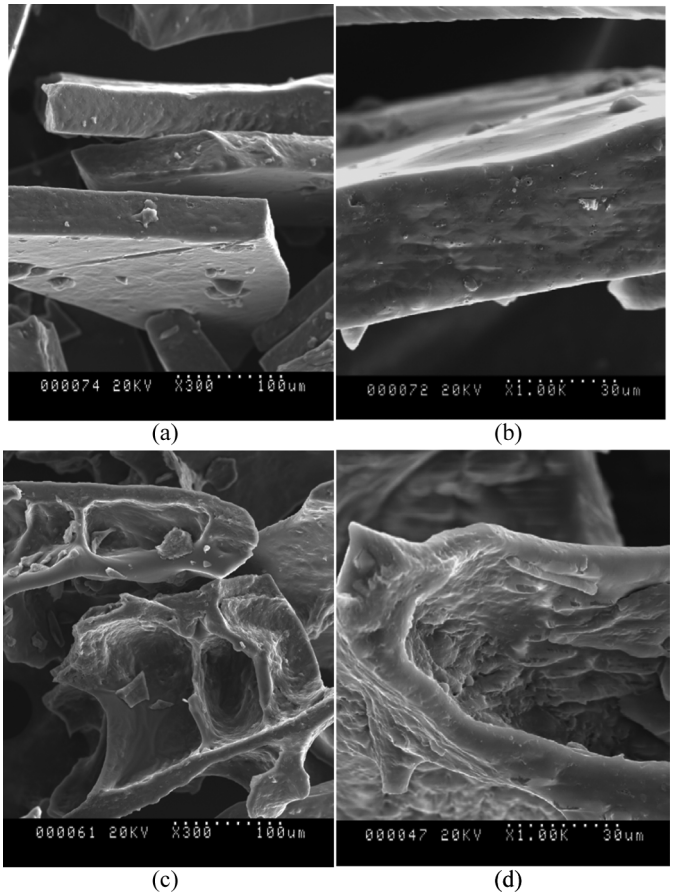

(a) (b) (c) (d)

FIG. 6. Scanning electron micrographs (SEM) of mango powders (180–250 μm) dried using Refractance Window drying (a & b) and freeze drying (c & d) at magnification of 300× (a & c) and 1,000× (b & d), 20 kV.[13]

can be observed only when the drying temperature applied is above the glass transition temperature of the material at a given water content. Rahman[39] also explained the concept of glass transition and its relationship to pore formation. According to that study by Rahman,[39] more pores or negligible collapse can be observed when a material is dried below T_g, while fewer pores can be observed when processed at $T > T_g$. The onset glass transition temperature of RW- and freeze-dried mango powder solids was 30.6 ± 1.5°C and 33.4 ± 3.4°C, respectively (Table 3). As shown in Fig. 6, the mango powder obtained by freeze drying at a plate temperature of 20 ± 1°C ($T < T_g$) formed large pores, while the application of higher temperature of 74 ± 2°C during RW-drying ($T > T_g$) resulted in a more rigid product with lower porosity. The above hypothesis therefore supports our observations. Other studies have revealed that products obtained by freeze drying at $T < T_g$ were in the glassy state, have negligible shrinkage, and hence are very porous when compared to those that are processed by hot-air drying ($T > T_g$), which are rubbery and are prone to collapse and shrinkage.[11,36]

Individual particles of mango powders obtained by RW and freeze-drying processes were further examined using a scanning electron microscope at higher magnification. The RW-dried mango powder clearly showed a composite sheet with distinguishable internal pores along the cross-section of each particle, indicating that some empty spaces formed during evaporation were not replaced as the mango puree was dried (Fig. 6a,b). On the other hand, visual observation of freeze-dried mango powder revealed larger pores for every single particle (Fig. 6c,d). This further explains why the porosity of freeze-dried materials was always higher in comparison with other drying methods.

CONCLUSIONS

The sorption isotherms for RW- and freeze-dried mango powders showed sigmoidal characteristics type III (J-shape) when fitted to both GAB and BET models. This was attributed to the highly porous and hygroscopic nature of freeze-dried mango powder compared to RW-dried powder. The GAB monolayer water content (M_g) obtained for RW- and freeze-dried mango powder was 0.078 kg H_2O/kg dry solids and 0.045 kg H_2O/kg dry solids, respectively. These are within the range of 0.029–0.11 kg H_2O/kg dry solids reported for several dehydrated foods. Both the onset glass transition (T_{gi}) of RW- and freeze-dried mango powder solids decreased as the water activity increased. There were no significant differences in T_{gi} of RW-dried and freeze-dried mango powder solids at constant water activities, except for $a_w = 0.86$. The glass transition temperature for RW- and freeze-dried mango powder solids at zero water (T_{gs}), when fitted to the Gordon-Taylor model, was 55.82 and 63.61°C, respectively. Microscopic examination of the mango powders showed that RW-dried mango powder was smooth and flaky with nearly uniform thickness, while freeze-dried mango powder showed a skeletal structure with large pores. The results generated provide valuable information for predicting the stability of RW- and freeze-dried mango powders.

ACKNOWLEDGMENTS

This study was supported by the Ford Foundation International Fellowship Program (IFP)-Philippines and IFP/Institute of International Education, New York. We thank the Philippine Center for Postharvest Development and Mechanization (PhilMech) for granting study leave to author Ofero Caparino. Special thanks to Richard E. Magoon and Karin M. Bolland (MCD Technologies, Inc., Tacoma, WA) for allowing the use of their RW drying facilities and for their assistance with the experiments; Engr. Frank Younce for technical assistance on the operation of the freeze dryer; and Dr. Valerie Lynch-Holm for helping with SEM imaging.

REFERENCES

1. BAS. Situation Report on Selected Fruit Crops, 2009. http://www.bas.bas.gov (accessed March 1, 2011).
2. Rajkumar, P.; Kailappan, R.; Viswanathan, R.; Raghavan, G.S.; Ratti, C. Foam mat drying of alphonso mango pulp. *Drying Technology* **2007**, *25*, 357–365.
3. Bhandari, B.R.; Datta, N.; Howes, T. Problems associated with spray drying of sugar-rich foods. *Drying Technology* **1997**, *15*(2), 671–684.
4. Rahman, M.S.; Labuza, T.P. Water activty and food preservation. In *Handbook of Food Preservation*; Rahman, M.S., Ed.; Marcel Dekker, Inc.: New York, 1999; 339–382.
5. Karel, M. Freeze dehydration of foods. In *Principles of Food Science*; Karel, M., Fennema, O.R., Lund, D.B., Eds.; Marcel Dekker, Inc.: New York, 1975; 359–395.
6. Rahman, M.S. State diagram of foods: Its potential use in food processing and product stability. *Trends in Food Science & Technology* **2006**, *17*, 129–141.
7. Slade, L.; Levine, L. A food polymer science approach to structure property relationships in aqueous food systems: Non-equilibrium behaviour of small carbohydrate-water system. In *Water Relationships in Food*; Levine, L., Slade, L., Eds.; Plennum Press: New York 1991.
8. Roos, Y. Water activity and glass transition temperature. In *Food Preservation by Moisture Control: Fundamentals and Applications*; Barbosa-Canovas, G.V., Welti-Chanes, J., Eds.; Technomic: Lancaster, PA, 1995; 133–154.
9. Sablani, S.S.; Syamaladevi, R.M.; Swanson, B.G. A review of methods, data and applications of state diagram of food systems. *Food Engineering Review*, **2010**, *2*, 168–203.
10. Syamaladevi, R.M.; Sablani, S.S.; Tang, J.; Powers, J.; Swanson, B.G. State diagram and water adsorption isotherm of raspberry (Rubus Idaeus). *Journal of Food Engineering*, **2009**, 460–467.
11. Sablani, S.S.; Kasapis, S.; Rahman, M.S. Evaluating water activity and glass transition concepts for food stability. *Journal of Food Engineering* **2007**, *78*, 266–271.
12. Rahman, M.S. *Food Properties Handbook*; CRC Press: Boca Raton, FL, 1995.
13. Caparino, O.A.; Tang, J.; Nindo, C.I.; Sablani, S.S.; Powers, J.R.; Fellman, J.K. Effect of drying methods on the physical properties

and microstructures of mango (Philippine carabao var.) powder. *Journal of Food Engineering*, **2012**, *111*, 135–148.
14. Nindo, C.I.; Tang, J. Refractance Window dehydration technology: A novel contact drying method. *Drying Technology* **2007**, *25*, 37–48.
15. Barbosa-Canovas, G.V.; Ortega-Rivas, E.; Juliano, P.; Yan, H. *Food Powders: Physical Properties, Processing, and Functionality*; Kluwer Academic/Plenum Publishers: New York, 2005.
16. AOAC. *Official Methods of Analysis*; Association of Official Analytical Chemists: Washington, DC, USA, 1998.
17. Spiess, W.E.L.; Wolf, W. 1987. Critical evaluation of methods to determine moisture sorption isotherms. In *Water Activity: Theory and Applications to Foods*; Rockland, L.B., Beuchat, L.R., Eds.; MarcelDekker: New York, 1987; 215–234.
18. Brunauer, S.; Emmett, P.H.; Teller, E. Adsorption of gases in multimolecular layers. *Journal of American Chemists' Society* **1938**, *62*, 309–319.
19. Henderson, S. A basic concept of equilibrium moisture. *Agricultural Engineering* **1952**, *33*, 29–32.
20. Rockland, L.B.; Stewart, G.F. *Water Activity: Influence of Food Quality*; Academic Press: New York, 1981.
21. Labuza, T.P. Sorption phenomena in foods. *Journal of Food Technology* **1968**, *22*(3), 15–24.
22. Bizot, H. Using the GAB model to construct sorption isotherms. In *Physical Properties of Foods*; Jowitt, R., Escher, F., Hallstrom, B.M., Spiess, W.E., Vos, G., Eds.; Applied Science: London, 1983; 42–54.
23. Falade, K.O.; Aworth, O.C. Adsorption isotherms of osmo-oven dried African star apple (Chrysophyllum albidum) and African mango (Irvingia gabonensis) slices. *Eur Food Res Technology* **2004**, *218*, 278–283.
24. Labuza, T.; Altunakar, B. Water activity prediction and moisture sorption isotherms. In *Water Activity in Foods: Fundamentals and Applications*; Barbosa-Canovas, G.V., Fontana, A.J., Eds.; Blackwell Publishing: Ames, Iowa, 2007; 109–154.
25. Lim, L.T.; Tang, J.; He, J. Moisture sorption characteristics of freeze-dried blueberrries. *Journal of Food Science* **1995**, *60*, 810–814.
26. Fabra, M.J.; Talens, P.; Moraga, P.; Martinez-Navarrete, N. Sorption isotherm and state diagram of grapefruit as a tool to improve product processing and stability. *Journal of Food Engineering* **2009**, *93*, 52–58.
27. Jakubczyk, E.; Ostrowska-Ligeza, E.; Gonde, E. Moisture sorption characteristics and glass transition temperature apple puree powder. *International Journal of Food Science and Technology* **2010**, *45*, 2515–2523.
28. Rangel-Marron, M.; Welti-Chanes, J.; Cordova-Quiros, A.V.; Ceron-Breton, J.G.; Ceron-Breton, R.M.;Anguebes-Fransechi, F. Estimation of sorption isotherms of mango pulp freeze-dried. *International Journal of Biology and Biomedical Engineering* **2011**, *5*(1), 18–23.
29. Yu, L.; Mazza, G.; Jaya, D.S. Moisture sorption characteristics of freze-dried, osmo-freeze-dried and 0smo-air-dried cherries and bluberries. *Transactions of the ASAE* **1999**, *42*(1), 141–147.
30. Roos, Y.H.; Karel, M. Phase transition of amorphous sucrose and sucrose solution. *Journal of Food Science* **1991a**, *56*, 266–267.
31. Bhandari, B.R. Implication of glass transition for the drying and stability of dried products. *Journal of Food Engineering* **1999**, *40*(1–2), 71–79.
32. Telis, V.R.; Sobral, P.J. Glass transition of freeze-dried and air-dried tomato. *Food Research International* **2002**, *35*, 435–443.
33. Roos, Y.H. Effect of moisture on the thermal behavior of strawberries studied using differential scanning calorimetry. *Journal of Food Science* **1987**, *1*, 146–149.
34. Jaya, S.; Das, H. Glass transition and sticky point temperatures and stability/mobility doagram of fruit powders. *Food Bioprocess Technology* **2009**, *2*, 89–95.
35. Roos, Y.H.; Karel, M. Plasticizing effect of water on thermal behaviour and crystallization of amorphous food models. *Journal of Food Science* **1991b**, *56*, 38–43.
36. Krokida, M.K.; Maroulis, Z.B. Effect of drying method on shrinkage and porosity. *Drying Technology* **1997**, *15*(10), 2441–2458.
37. Krokida, M.K.; Karathanos, V.T.; Maroulis, Z.B. Effect offreeze-drying conditions on shrinkage and porosity of dehydrated agricultural products. *Journal of Food Engineering* **1998**, *35*, 369–380.
38. Achanta, S.; Okos, M.R. Predicting the quality of dehydrated foods and biopolymers: Research needs and opportunities. *Drying Technology* **1996**, *14*(6), 1329–1368.
39. Rahman, M.S. Toward prediction of porosity in foods during drying: A brief review. *Drying Technology* **2001**, *19*(1), 1–13.
40. Ferrari, C.C.; Germer, S.P.M.; Alvim, I.D.; de Aguirre, J.M. Storage stability of spray-dried blackberry powder produced with maltodextrin or Gum Arabic. *Drying Technology* **2013**, *31*(4), 470–478.
41. Palzer, S.; Dubois, C.; Gianfrancesco, A. Generation of product structures during drying of food products. *Drying Technology* **2012**, *30*(1), 97–105.
42. Mrad, N.D.; Bonazzi, C.; Boudhrioua, N.; Kechaou, N.; Courtois, F. Moisture sorption isotherms, thermodynamic properties, and glass transition of pears and apples. *Drying Technology* **2012**, *30*(13), 1397–1406.
43. Torezan, G.A.P.; Menezes, H.C.; Katekawa, M.E.; Silva, M.A. Microstructure and adsorption characteristics of mango chips obtained by osmotic dehydration and deep fat frying. *Drying Technology* **2007**, *25*(1–3), 153–159.
44. Witrowa-Rajchert, D.; Rzaca, M. Effect of drying method on the microstructure and physical properties of dried apples. *Drying Technology* **2009**, *27*(7–8), 903–909.
45. Talla, A.; Jannot, Y.; Nkeng, G. E.; Puiggali, J. R. Experimental determination and modeling of sorption isotherms of tropical fruits: Banana, mango, and pineapple. *Drying Technology* **2005**, *23*(7), 1477–1498.